

Application of Dynamic Model for Wheeled Undercarriage of Earthmoving Machine to Simulate Its Ride

Melichar Kopas¹

Eva Faltinová²

Martin Mantič³

Jozef Kuľka⁴

¹ Faculty of Mechanical Engineering, The Technical University of Košice, Letná 9, 042 00 Košice, Slovak Republic. E-mail: melichar.kopas@tuke.sk

² Faculty of Mechanical Engineering, The Technical University of Košice, Letná 9, 042 00 Košice, Slovak Republic. E-mail: eva.faltinova@tuke.sk

³ Faculty of Mechanical Engineering, The Technical University of Košice, Letná 9, 042 00 Košice, Slovak Republic. E-mail: martin.mantic@tuke.sk

⁴ Faculty of Mechanical Engineering, The Technical University of Košice, Letná 9, 042 00 Košice, Slovak Republic. E-mail: jozef.kulka@tuke.sk

Grant: VEGA 1/0198/15

Název grantu: Research of innovative methods for emission reduction of driving units used in transport vehicles and optimisation of active logistic elements in material flows in order to increase their technical level and reliability.

Oborové zaměření: JR Other engineering

© GRANT Journal, MAGNANIMITAS Assn.

Abstract: This paper deals with creation of a dynamic model, which describes wheeled undercarriage of earthmoving machine, namely the mobile articulated machine, in order to develop elements for steering mechanism. There are implemented in this dynamic model the real forces acting on the undercarriage during driving through the defined testing corridor. The computational part of this article presents the basic mathematical description of the undercarriage dynamic behaviour and it enables to perform simulation of driving process.

Keywords: dynamic model, wheeled undercarriage, articulated wheel loader, control of drive direction.

1. INTRODUCTION

Research in the dynamics of mobile working machines, especially the earthmoving machines, uses dynamic model simulation with concentrated mass. Mass is concentrated in the center of gravity of those vehicle parts that can perform mutually independent movements.

Mobile working machines or the earthmoving machines with an articulated frame comprises two parts, which are interconnected by an articulation joint with two degrees of freedom.

The use of the horizontal joint that enables independent movements of the individual machine sections in relation to its longitudinal axis of symmetry makes the frame statically determinate. At the same time, however, the joint causes an increase in the number of independent coordinates, which describe the system's position and a reduction in the stability of travel on the slope.

Both axles are rigid, unsuspended and they have the identical track widths. Two linear hydraulic motors mutually control steering of both sections around the articulated joint. During linear motion, the back axle wheels move in the front wheel axle track, which decreases rolling resistance and thus also power consumption necessary for travel.

Since the axles are unsuspended, tires are the only suspension elements, which are affected by the kinematic excitation caused in the system by traveling on uneven surfaces. To perform a detailed solution to concerns over steering stability and to analyze the dynamics of cornering performance, it would be beneficial to also consider the stiffness of linear hydraulic motors and the hydraulic power circuit (pipe and hose stiffness, hydraulic fluid characteristics and so on), which would however considerably complicate the resulting dynamic model.

2. UNDERCARRIAGE OF ARTICULATED LOADER

In order to design the undercarriage, drive and steering system or to investigate the dynamic undercarriage properties, it is necessary to know the nature and magnitude of the acting forces.

To create a dynamic model, we follow the requirements for the structure of the machine and the valid technical standards.

The conditions for verifying the properties of the undercarriage control mechanisms in the earthmoving machines are defined by the STN EN 12643 [10].

The required dimensions of the test track for building machines and agricultural machines are presented in Fig. 1, where:

A = 1.1-times of the turning circle or 14 m, the larger value of the two is used,

B = 1.75-times of the turning circle or 22 m, the larger value of the two is used,

C = 2-time of the maximum wheelbase or 15 m, the smaller value of the two is used.

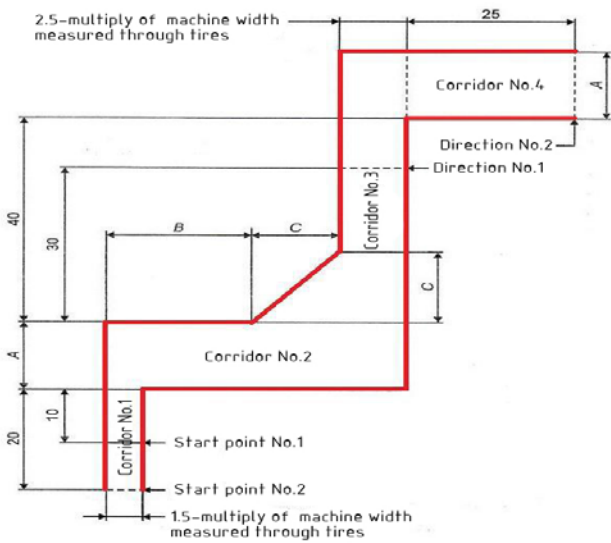


Fig. 1 Shape of a standard test corridor

It is suitable to choose the shape of the test track for movement simulation during the investigation of loading forces. The vehicle performs a manoeuvre along the designated course at a constant speed of $16 \text{ km.h}^{-1} \pm 2 \text{ km.h}^{-1}$.

The articulated wheel loader model (Fig.2) was created using the software product SolidWorks to preserve the weight and the position of the centers of gravity for the individual structural groups.

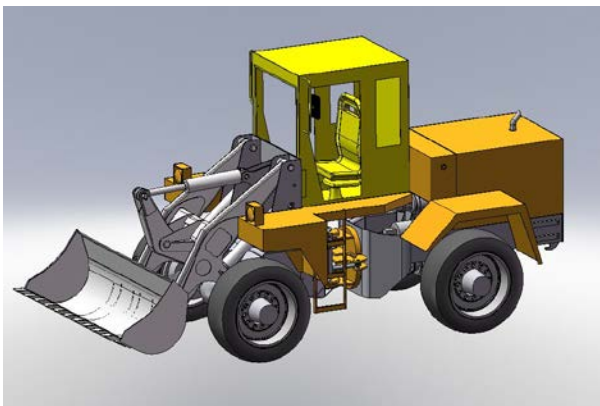


Fig. 2 Three-dimensional model of an articulated wheel loader

In terms of the physical and mechanical properties that significantly affect its properties, the wheel loader model comprises the following:

- solid physical bodies,
- suspension elements,
- speed control system,
- steering system.

2.1 Dynamic model of an articulated loader undercarriage

During design, the model involved 35 main structural elements. It, however, proved too extensive and placed great demands on computer performance, operation memory and solution time. It is suitable to replace it with a dynamic model with concentrated

masses (Fig.3). Weight characteristics can be defined by means of a suitable CAD software product.

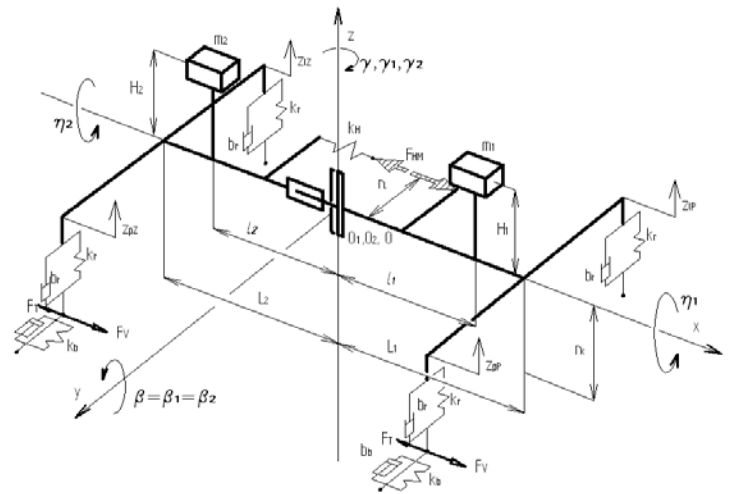


Fig. 3 Dynamic model of an articulated loader with concentrated masses

Suspension elements in the model include tires and the steering system. It is suitable to choose a cylindrical tire shape, which adequately characterizes the interaction between the wheel and the track surface. Replacing the tire shape with a torus could cause a discontinuity during networking, which induces additional harmonic excitation in the undercarriage during ride simulation. For this reason, a tire is often replaced by a suspension ring with a set of radial linear springs and viscous dampeners installed in parallel. (Fig.4) The magnitude of the force in the springs is proportional to the magnitude of deformation and the magnitude of the damping force is proportional to the deformation speed.

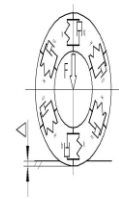


Fig.4 Alternate dynamic wheel model

2.2 Steering

There are many structural design variants of the steering mechanisms. Their selection depends on the need to position the vehicle precisely, but mostly on the value of forces, which affect the undercarriage. Control systems are described in greater detail in [1] and [4].

The simplest steering principle involves using two 2-stroke linear hydraulic motors and a vertical joint (Fig.5).

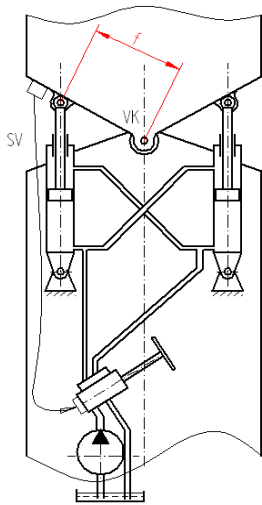


Fig.5 Scheme of hydraulic interconnection between the linear hydraulic motors
 VK – vertical joint, SV – return valve

This particular structural solution, however, causes a statically indeterminate coupling, which the computational simulation program does not accept. We can resolve this concern by introducing a virtual linear hydraulic motor steering system. Once the required breakaway torque, which is needed for a change of direction, is detected, it is possible to perform a reverse transformation to the forces acting in the individual real-world hydraulic motors. At the same time, we assume that the magnitude of forces is proportional to the active surface area of the piston.

3. INFLUENCE OF UNDERCARRIAGE CONTROL ON RIDE DYNAMICS

A curved travel of the vehicle is a motion of the vehicle on the curved trajectory around the instantaneous centre of the wheel loader rotation O1. The point O1 is a cross point of the prolonged axles according to Fig.6.

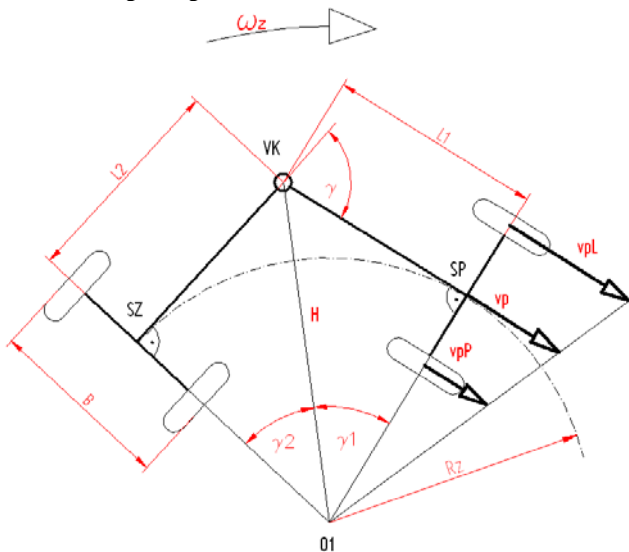


Fig.6 Curved travel, horizontal projection

Explanation of the symbols used in Fig.6 are as follows:

- O1 – instantaneous centre of the wheel loader rotation;
- SP – centre of the front axle;
- SZ – centre of the rear axle;
- VK – vertical hinge;
- L1, L2 – distances of axles from the vertical hinge;
- B – wheel track;
- R_z - instantaneous turning radius;
- ω_z - angular speed relating to the centre of rotation

Thus, the vehicle turning is caused by a mutual turning of the front and rear part of the wheel loader around the vertical hinge VK.

In a case of the constant travelling speed v_p , the circumferential speed of the wheels on both sides of the vehicle will be different during a curved travel.

Let the circumferential speed of the wheel, which is situated on the internal side of curve, is signed v_{pP} and the circumferential speed of the wheel rotating on the external side of curve is signed v_{pL} . It is evident that $v_{pL} > v_{pP}$.

The travel speed of the loader can be expressed as follows

$$v_p = \omega_z R_z, \tag{1}$$

ω_z - is the angular speed relating to the centre of rotation,

R_z - is the instantaneous turning radius.

Then the circumferential speed v_{pP} of the wheel, which is situated on the internal side of curve, can be written in the form

$$v_{pP} = \omega_z \left(R_z - \frac{B}{2} \right) \tag{2}$$

and the circumferential speed v_{pL} of the wheel on the external side of curve will be

$$v_{pL} = \omega_z \left(R_z + \frac{B}{2} \right). \tag{3}$$

In the case of the cranked loader configuration, the turning angle between the front and rear part of the vehicle is γ (Fig.6), whereas

$$\gamma = \gamma_1 + \gamma_2, \tag{4}$$

γ_1 - is the turning angle of the loader front part,

γ_2 - is the turning angle of the loader rear part.

According to the right triangles $\Delta(O1,SP,VK)$ and $\Delta(O1,SZ,VK)$ the length of hypotenuse H is $H = \frac{L_1}{\sin \gamma_1}$ as well as $H = \frac{L_2}{\sin \gamma_2}$,

see Fig.3.

By comparison of the both relations, which are valid for the value H of the hypotenuse length, there is obtained the equation

$$\frac{L_1}{\sin \gamma_1} = \frac{L_2}{\sin \gamma_2}, \quad (5)$$

and from this equation (5) it is

$$\sin \gamma_2 = \frac{L_2}{L_1} \sin \gamma_1, \quad (6)$$

Since $\gamma = \gamma_1 + \gamma_2$ then $\gamma_2 = \gamma - \gamma_1$ and the equation (6) is modified as follows

$$\sin(\gamma - \gamma_1) = \frac{L_2}{L_1} \sin \gamma_1. \quad (7)$$

The relation (7) can be rewritten by means of the well-known goniometric rule $\sin(\alpha - \beta) = \sin \alpha \cos \beta - \cos \alpha \sin \beta$ into the next form

$$\sin \gamma \cos \gamma_1 - \cos \gamma \sin \gamma_1 = \frac{L_2}{L_1} \sin \gamma_1. \quad (8)$$

After an adjustment of the equation (8) there is

$$\frac{\sin \gamma}{\operatorname{tg} \gamma_1} - \cos \gamma = \frac{L_2}{L_1}. \quad (9)$$

The relation, which is valid for the $\operatorname{tg} \gamma_1$, is obtained from the (9)

$$\operatorname{tg} \gamma_1 = \frac{\sin \gamma}{\frac{L_2}{L_1} + \cos \gamma}. \quad (10)$$

Simultaneously, according to Fig.6, from the triangle $\Delta(O1,SP,VK)$ it follows,

$$\operatorname{tg} \gamma_1 = \frac{L_1}{R_z}. \quad (11)$$

By comparison of the left sides from the equations (10) and (11) there is obtained the next relation

$$\frac{L_1}{R_z} = \frac{\sin \gamma}{\frac{L_2}{L_1} + \cos \gamma} \quad (12)$$

and from the equation (12) it can be determined the value of the instantaneous turning radius R_z

$$R_z = \frac{L_2 + L_1 \cos \gamma}{\sin \gamma}. \quad (13)$$

From the equation (1) it is following

$$\omega_z = \frac{v_p}{R_z}. \quad (14)$$

The circumferential speed v_{pP} of the wheel, which is situated on the internal side of curve as well as the circumferential speed v_{pL} of the wheel on the external side, can be obtained after setting of the relation (14) into the equations (2) and (3), as follows

$$v_{pP} = v_p \left(1 - \frac{B \cdot \sin \gamma}{2 \cdot (L_2 + L_1 \cos \gamma)} \right), \quad (15)$$

$$v_{pL} = v_p \left(1 + \frac{B \cdot \sin \gamma}{2 \cdot (L_2 + L_1 \cos \gamma)} \right). \quad (16)$$

At the same time it is valid that

$$v_{pP} = r_k \omega_{pP} \text{ and } v_{pL} = r_k \omega_{pL},$$

r_k – is the dynamic wheel radius.

Thus, the values of the angular speed ω_{pP} of the of the wheel, which is situated on the internal side and the angular speed ω_{pL} of the external side wheel are

$$\omega_{pP} = \frac{v_p}{r_k} \left(1 - \frac{B \cdot \sin \gamma}{2 \cdot (L_2 + L_1 \cos \gamma)} \right), \quad (17)$$

$$\omega_{pL} = \frac{v_p}{r_k} \left(1 + \frac{B \cdot \sin \gamma}{2 \cdot (L_2 + L_1 \cos \gamma)} \right). \quad (18)$$

According to the above-mentioned equations (17) and (18), there is evident a significant difference between the angular speed values of the wheels rotating on the both sides of axle.

This fact corresponds to the function of the axle differential of the given wheel loader, whereas the relations (17) and (18) are representing analytical description of its function.

4. CONCLUSION

There is presented in this article a methodology, which is applied for development of a dynamic model of the wheeled undercarriage for the earthmoving machine, namely the articulated wheel loader. This methodology creates assumptions for simulation and analysis of mobile vehicle driving abilities.

The analysis of kinematic relations occurring during the driving process is a basic assumption, which is necessary for creation of the resulting dynamic model of the wheeled undercarriage for a mobile working machine [4].

The equations (17) and (18) are the final result of the performed kinematic analysis of the loader travel in a curve. These equations are useful for the next process of vehicle travel simulation.

This paper was elaborated in the framework of the projects VEGA 1/0198/15 Research of innovative methods for emission reduction of driving units used in transport vehicles and optimisation of active logistic elements in material flows in order to increase their technical level and reliability and KEGA 021TUKE – 4/2015 Development of cognitive activities focused on innovations of educational programs in the engineering branch, building and modernisation of specialised laboratories specified for logistics and intra-operational transport.

Sources

1. Dudzinski Piotr. 2005. *Lenksysteme fuer Nutzfahrzeuge*. Berlin: Springer-Verlag. ISBN 3-540-22788-1.
2. Kučík Pavol, Igor Strážovec, Peter Kriššák. 2000. *Hydraulický prenos energie. Mobilné pracovné stroje*. Žilina: EDIS-ŽU. ISBN 80-7100-725-0.
3. Kunze Günter, Helmut Göhring Klaus JACOB. 2002. *Baumaschinen. Erdbau - und Tagebaumaschinen*. Braunschweig: Vieweg und Sohn. ISBN 3-528-06628-8.
4. Heisler Heinz. 2002. *Advanced Vehicle Technology*. Warrendale: SAE International. ISBN-9780080493442.
5. Findeisen Dietmar. 2006. *Ölhydraulik. Handbuch für die hydrostatische Leistungsübertragung in der Fluidtechnik*. Berlin: Springer-Verlag. ISBN 13 978-3-540-23880-5.
6. Vaško M., Leitner B., Sága M. 2010. *Computational Fatigue Damage Prediction of the Lorry Frames Under Random Excitation*. Communications 12(4): 62–67. ISSN 1335–4205.
7. Sága M., Kopas P., Vaško M. 2010. *Some Computational Aspects of Vehicle Shell Frames Optimization Subjected to Fatigue Life*. Communications 12(4): 73–79. ISSN 1335–4205.
8. Konieczny Ł., Burdzik R., Warczek J., Czech P., Wojnar G., Młyńczak J. 2015. *Determination of the effect of tire stiffness on wheel accelerations by the forced vibration test method*. Journal of Vibroengineering 17(8): 4469-4477. ISSN 1392-8716.

9. Dekys V., Sapietova A., Stevka O. 2013. Understanding of The Dynamical Properties of Machines Based on The Interpretation of Spectral Measurement and FRF. In. *51st International Scientific Conference "Experimental Stress analysis"*: 106-112. Litomerice, Czech Republic. 11-13 June 2013.

10. STN EN 12643. *Stroje na zemné práce. Stroje na kolesovom podvozku. Požiadavky na systémy riadenia*. 1997.

11. Izrael G., Bukoveccky J., Gulan L. 2011. Utilisation of modeling, stress analysis, kinematics optimisation, and hypothetical estimation of lifetime in the design process of mobile working machines. In *Scientific Proceedings Faculty of Mechanical Engineering STU Bratislava* 19(2011):23-28. ISSN 1338-1954.